J Solid State Electrochem (2012) 16:3499–3504
DOI 10.1007/s10008-012-1799-z

ORIGINAL PAPER

Some critical factors for photocatalysis on self-organized TiO_2 nanotubes

Ning Liu · Indhumati Paramasivam · Min Yang · Patrik Schmuki

Received: 15 April 2012 / Revised: 8 June 2012 / Accepted: 13 June 2012 / Published online: 29 June 2012

Abstract In the present work, different intrinsic and extrinsic parameters are investigated that affect the photocatalytic activity of self-organized TiO_2 nanotube layers. Particularly, the influence of annealing temperature and annealing atmosphere, the influence of different gas purging in the electrolyte, and the effect of applied voltage on the photocatalytic degradation rates of acid orange (AO7) are discussed. We find that the effect of the reducing gas atmosphere dominates over the anatase/rutile ratio in activating the nanotube layers. Moreover, we show that the effect of different gas purging (Ar and O_2) of the electrolyte affects the reaction rate twofold: (1) by providing electron acceptor states and also by (2) a different change in the red–ox potential, i.e., the band bending in TiO_2. By an external anodic voltage, the reaction rates can be increased drastically due to increased band bending. Nevertheless, the magnitude of the effect is also affected by the presence or absence of O_2 in the electrolyte.

Keyword Photocatalysis · TiO_2 nanotubes · Crystalline phase · Charge transfer

Introduction

Ever since the first report by Fujishima and Honda in 1972 [1] that found TiO_2 to be an excellent photocatalyst, this material has attracted a high interest for degradation of various organic compounds [2–6]. The reaction sequence is based on UV-induced electron–hole pair formation in semiconducting TiO_2 ($E_{g,\ anatase}$ = 3.2 eV; $E_{g,\ rutile}$ = 3.0 eV) where the photogenerated electrons react in aqueous environments, typically with an electron capture agent such as O_2 (or H_2O) while the holes when ejected to water may create O_2 or $OH^{\bullet}$ radicals. Both radical reaction products, i.e., via the electron path $O_2^{\bullet-}$ and via the hole path $OH^{\bullet}$, are considered to be highly reactive. In fact, the radical species are able to decompose virtually all organic materials such as pollutants or other reactants finally to CO_2 and H_2O. To achieve a high turnover rate, a high specific surface area of the TiO_2 material is desired and thus, for most conventional applications, TiO_2 nanoparticles are used either suspended in the solution or as immobilized compacted powder layers in various types of reactors [7, 8]. Nanoparticle layers that are coated on a conductive substrate can also be used as electrodes for photoelectrochemical applications, i.e., the photocatalytic activity can additionally be influenced with an applied electrochemical potential [1, 9, 10]. Recently, wide interest has been found on anodically grown self-organized TiO_2 nanotube layers for photocatalysis. As these layers are grown on a Ti substrate, they are directly back-contacted and thus very suitable as photoelectrodes [11, 12]. In certain cases, TiO_2 nanotube layers were found to possess, even under open-circuit conditions, a higher photocatalytic reactivity than nanoparticles [6], and earlier work indicated that, with an externally applied anodic bias, the photocatalytic performance of TiO_2 nanotubular layers could even be increased further [13, 14]—a general investigation on the photoelectrochemical behavior of various nanotubes is given in [15].

Over the years, a number of key factors that influence the photocatalytic performance of TiO_2 nanotube layers (such as tube length, diameter, and crystal structure) have been evaluated. A most crucial factor for the photocatalytic activity of the material is the crystalline phase [11]. For TiO_2 nanoparticles, the anatase phase is commonly believed to be superior, whereas the pure rutile phase shows a relatively lower photocatalytic

Dedicated to the 75th birthday of Prof. Waldfried Plieth

N. Liu · I. Paramasivam · M. Yang · P. Schmuki (✉)
Department of Materials Science WW4, LKO,
University of Erlangen—Nuremberg,
Martensstrasse 7,
91058 Erlangen, Germany
e-mail: schmuki@ww.uni-erlangen.de

activity [11, 16]. There are also a number of reports about synergistic effects in mixed phases of anatase and rutile in TiO_2 photocatalysis [17, 18]. Similar reactivity sequences have also been reported for TiO_2 nanotubes [19]. Nevertheless, hardly any attention has been paid to the oxidation state of TiO_2—i.e., if TiO_2 nanotubes are annealed under partially reducing or inert atmospheres. Therefore, we will address this point and other annealing aspects in the present work. Another often disregarded point in photocatalytic work using TiO_2 nanotubes is that under open-circuit conditions, in most aqueous systems, O_2 acts as the electron acceptor and this step is frequently considered as a rate-limiting step of the reaction, i.e., for TiO_2 nanoparticles in purely aqueous environment, holes are considered to react much faster with the solution than the conduction band electrons. In such a situation, the electron transfer from the TiO_2 to oxygen can be rate-controlling in photocatalytic processes [20, 21], and this step strongly depends on the band bending of the semiconductor electrolyte interface.

Therefore, we investigate in the present work the photocatalytic performance of self-organized TiO_2 nanotube layers under open-circuit potential (OCP) and applied potential conditions and considering O_2-saturated and -depleted conditions.

Experimental

As substrates for TiO_2 nanotube growth, Ti sheets (99.6 % purity, Advent Materials, UK) of 0.1-mm thickness were cleaned by sonication of the samples in acetone and ethanol, followed by rinsing with deionized (DI) water and drying in a nitrogen stream. To form TiO_2 nanotube layers, the metal foils were anodized using a high-voltage potentiostat (Jaissle IMP 88 PC) in a two-electrode configuration with platinum gauze as a counter-electrode in an electrolyte of 1 M Na_2SO_4 + 0.14 M NaF at 20 V for 1 h. Afterwards, the samples were immersed in DI water and then dried in a nitrogen stream. In order to investigate the influence of the crystal structure and oxidative state, the anodized samples were annealed in ambient air or argon at different temperatures for 3 h to produce a defined crystalline structure. Additionally, in order to explore a recently reported water annealing treatment [22], we immersed some samples according to the reported treatment in H_2O for 3 days and finally evaluated its photocatalytic activity. A field-emission scanning electron microscope (Hitachi FE-SEM S4800) was used for morphological characterization of the samples. The morphology of the nanotubes was obtained from scanning electron microscope (SEM) cross-sections. X-ray diffraction analysis (XRD) was performed with an X'pert Philips PMD with a Panalytical X'celerator detector using graphite-monochromatized Cu–K_α radiation.

For photocatalytic experiments, we followed a procedure described earlier [6, 23]. In brief, samples were immersed in a 10-mm quartz cuvette containing 3 ml Acid Orange (AO7), an azo dye ($C_{16}H_{11}N_2O_4SNa$, Acros Organics, Belgium) solution, of an initial concentration of 2.5×10^{-5} mol L^{-1}. After 1 h (to establish the dye adsorption/desorption equilibrium), we started to irradiate the samples with UV light using a 200-mW HeCd laser (I_{light} = 60 mW cm^{-2}, λ=325 nm, Kimmon, Japan) while

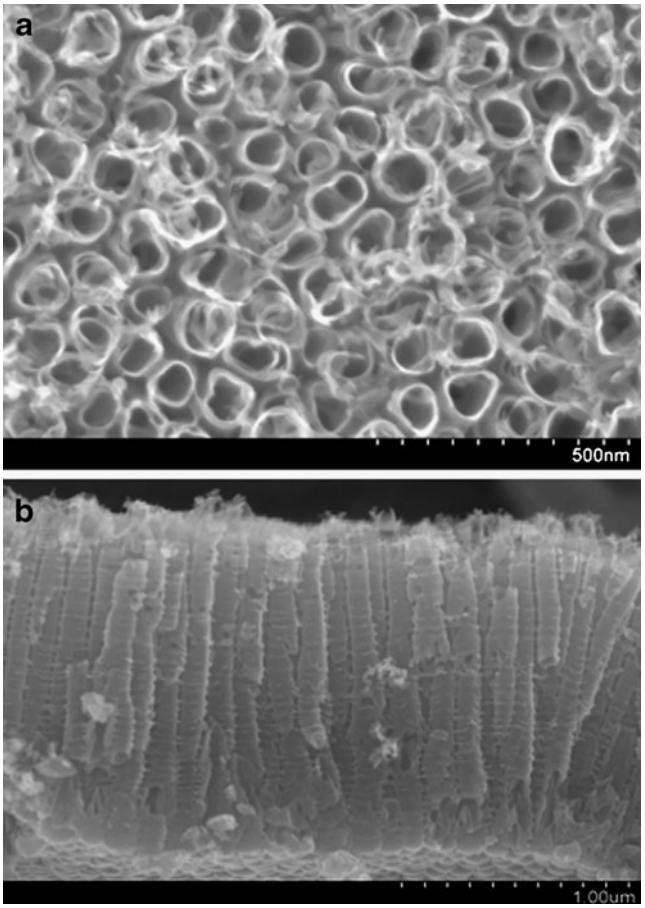

Fig. 1 SEM images of TiO_2 nanotubes in the top view (**a**) and in the cross-section (**b**)

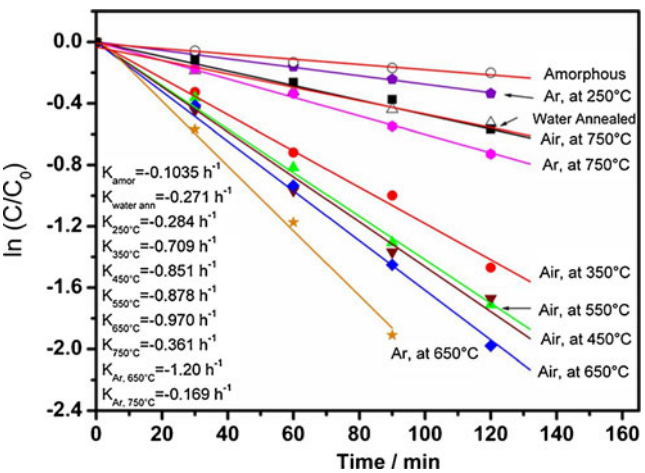

Fig. 2 Comparison of degradation curves of AO7 by TiO_2 nanotube layers after annealing at different temperatures and under different atmospheric conditions (air or Ar)

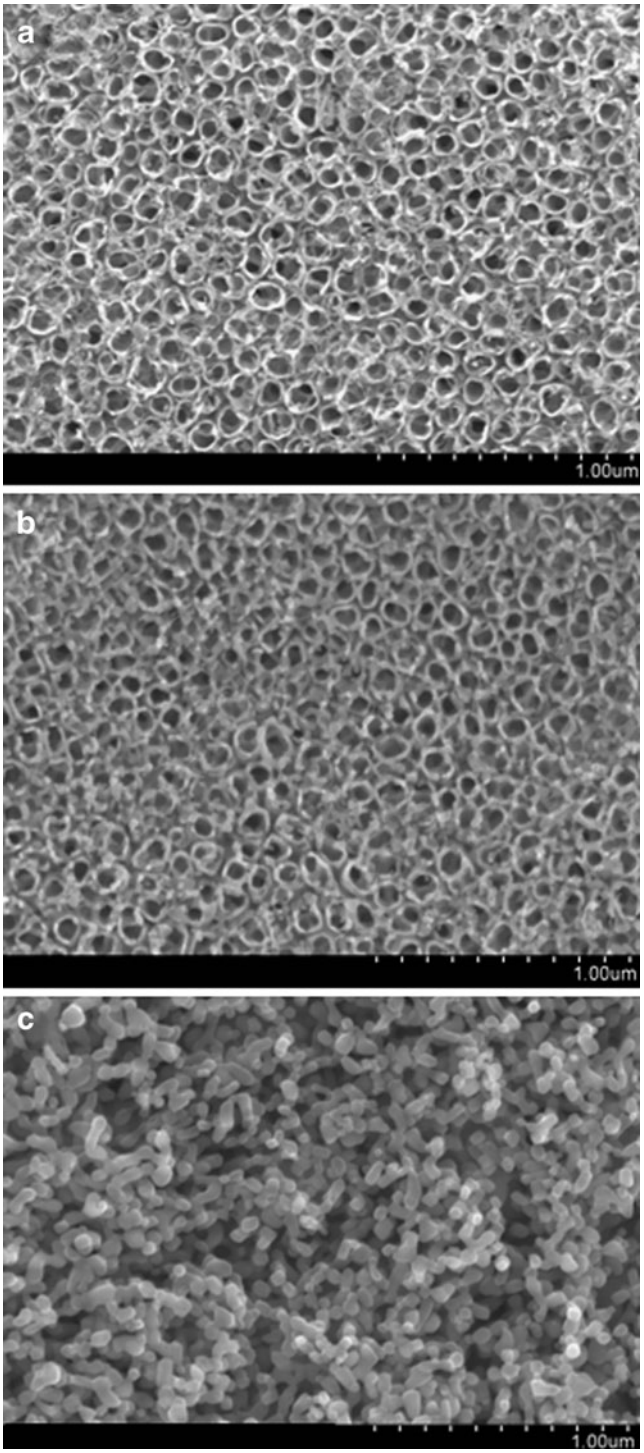

Fig. 3 SEM images of the surface morphology after annealing at different temperatures in air: **a** 450 °C, **b** 650 °C, **c** 750 °C

agitating the solution using a magnetic stirrer. In order to measure the decomposition rates of the dyes, the absorbance of the testing solution was measured periodically for AO7 absorbance every half an hour using a UV/vis spectrophotometer at a wavelength of λ=486 nm. In the atmospheric study, the solution was aerated by bubbling highly pure Ar or O_2 gas

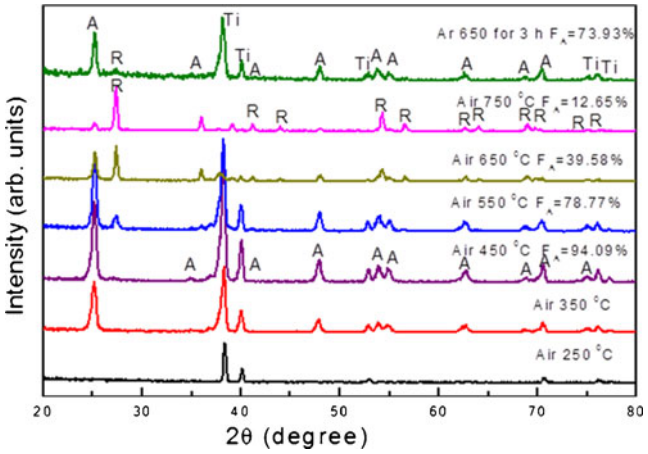

Fig. 4 XRD patterns of the TiO_2 nanotubes annealed in air at temperatures ranging from 250 to 750 °C for 3 h. *A* anatase, *R* rutile, *Ti* titanium

for about 20 min in the dark before irradiation, and Ar or O_2 gas purging was continued during irradiation.

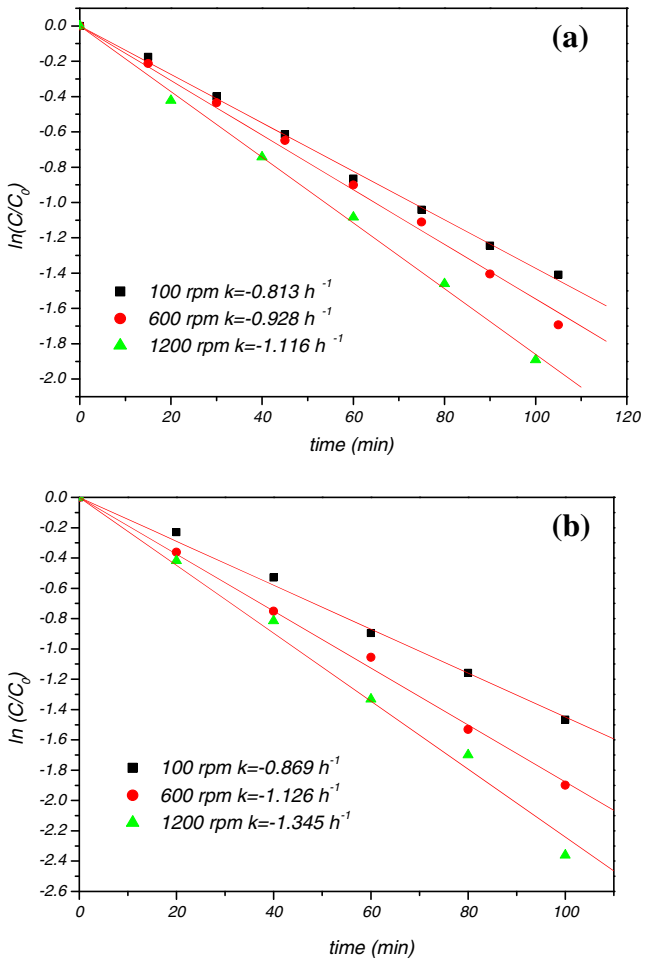

Fig. 5 Comparison of photocatalytic decomposition rates of AO7 by TiO_2 nanotubes (annealed at 450 °C in air) with different stirring rates under Ar (**a**) and O_2 (**b**) bubbling

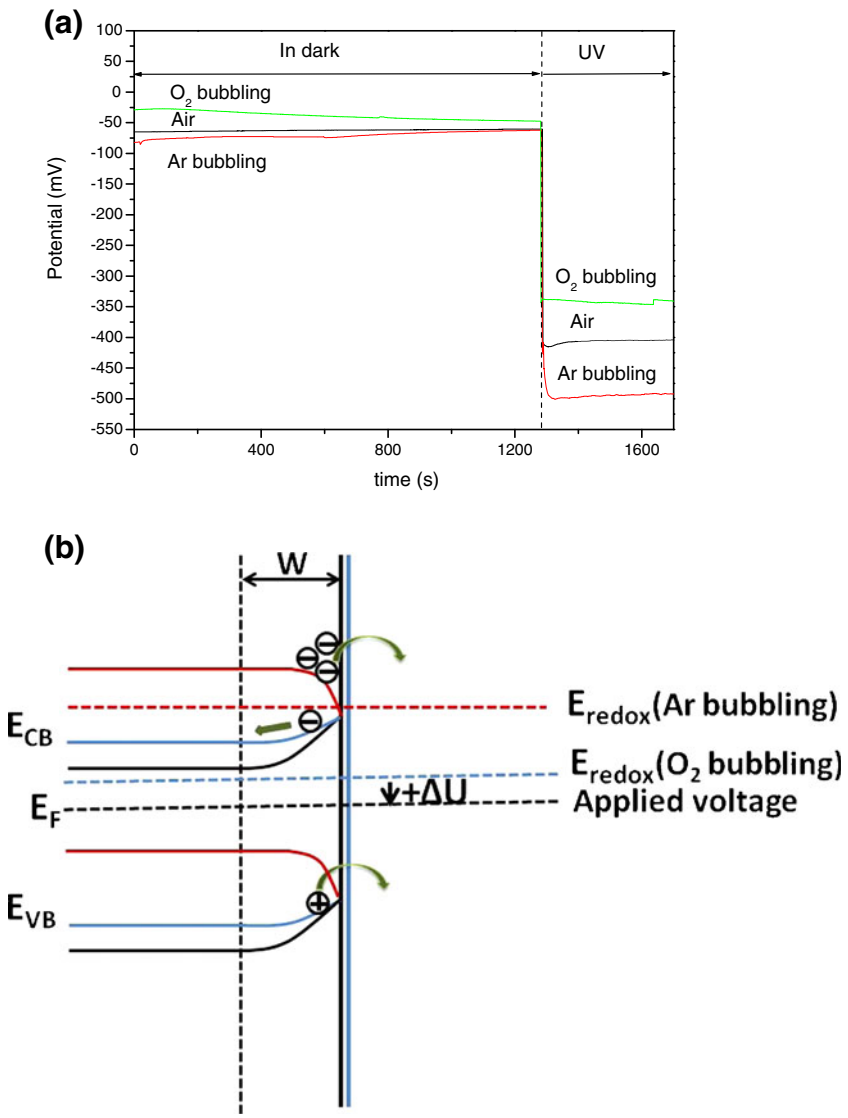

Fig. 6 OCP of the samples in AO7 solution (2.5×10^{-5} mol L^{-1}+0.1 mol L^{-1} Na_2SO_4) under O_2 and Ar bubbling in the dark and with UV illumination (**a**). Schematic illustration of energy levels in TiO_2 nanotube layer in the solution: with O_2 bubbling (depletion) and Ar bubbling (accumulation), applied anodic potential (stronger depletion) (**b**)

The open-circuit potential measurements and the electrochemically assisted photocatalytic measurements were carried out with a standard three-electrode cell by using a potentiostat (Jaissle Potentiostat 1030 DA). The TiO_2 samples, connected as a working electrode, were placed in a 20-mm quartz cell with 3-ml solution of 2.5×10^{-5} mol L^{-1} AO7 and 0.1 mol L^{-1} Na_2SO_4. The reference electrode was an Ag/AgCl electrode (3 M KCl), and platinum gauze was used as counter-electrode, which was separated in a glass frit compartment.

Results and discussion

Figure 1 shows SEM cross-sectional and top view images of tubular TiO_2 layer used in this work. The thickness of the layer is 1.5±0.1 μm, the tube wall thickness is in the range of 15–25 nm, and the tube diameter is 100±8 nm. In a first set of experiments, we evaluated the effect of different annealing treatments on the photocatalytic performance of these TiO_2 nanotubes. Figure 2 shows the degradation curves of AO7 for nanotube layers that were annealed in air at different temperatures. In line with previous work [24], with an increase of annealing temperature from 250 to 650 °C, the photocatalytic activity is enhanced. The highest photocatalytic activity is exhibited by TiO_2 nanotubes annealed at 650 °C. The samples annealed at 750 °C show a strongly decreased activity. Most remarkable is that a higher photocurrent can be achieved by partially reduced samples, i.e., clearly the sample annealed in Ar at 650 °C shows an even higher activity than the comparable air-annealed sample.

The surface morphology after annealing at different temperatures in air is shown in Fig. 3. The nanotube structure is found to be retained after annealing for 3 h at 650 °C

(Fig. 3a, b). No discernible changes in the pore diameter or wall thickness are observed for annealing temperatures ranging from 250 to 650 °C. At 750 °C, strong structural changes occur and the tubular layer is to a large extent collapsed as shown in Fig. 3c.

The change of the crystalline structure of the nanotubes upon annealing is shown in the XRD patterns of Fig. 4. The sample annealed at 250 °C is amorphous (only the reflections of titanium substrate are visible), while the 350-°C-annealed sample shows crystallization to anatase. Typically, annealing the TiO_2 nanotubes in air at temperatures higher than 280 °C leads to an anatase structure. For thermal annealing at 450 °C, an additional higher rutile peak emerges—this stems from a layer underneath the nanotubes (formed by thermal oxidation of the Ti metal substrates) [24]. With an increase of the annealing temperature, the magnitude of the rutile peaks increases, whereas the magnitude of the anatase peaks decreases. At 650 °C in air, rutile becomes the major constituent. However, even in the collapsed layer at 750 °C, there is still anatase present in TiO_2 layer.

From these findings, one can conclude that, for air annealing, a temperature of 650 °C exhibits the best catalytic performance. In literature, this has been explained by the synergistic effects of mixed phases of anatase and rutile [17–19, 24, 25]. However, if annealing is carried out in Ar atmosphere, at 650 °C an even higher degradation activity is obtained, although much less rutile has been formed than in air (Fig. 4). In other words, under these conditions, the anatase/rutile ratio cannot be responsible for the enhanced photocatalytic activity. In fact, under these reducing conditions (650 °C, Ar), deeply blue colored samples are formed due to their high Ti^{3+} content [26, 27]. Therefore, it seems more plausible to ascribe in this case the improved performance to the partially reduced state of these samples.

Another interesting aspect in the field of annealing nanotubes reports on improving the photocatalytic performance of nanotubes by water annealing treatment [22]. Therefore, for comparison, we also included a sample that was water-annealed for 3 days following literature procedures [22, 28]. From the results in Fig. 2, it is clear that these samples show an extremely low photocatalytic activity in comparison with thermal annealing. In a next set of experiment, we targeted some hardly considered aspects in electrochemical behavior when using TiO_2 nanotubes in photocatalysis.

Under open-circuit conditions, the charge transfer rate to dissolved oxygen is perceived as rate-determining. We therefore investigated the influence of O_2-saturated and -depleted electrolytes under different stirring rates on AO7 degradation. The results in Fig. 5 show rate constants measured in Ar or O_2 bubbling, indicating an acceleration of photocatalytic oxidation with increasing stirring speed, and acceleration under O_2-saturated conditions. Mechanical stirring usually affects photocatalytic reactions mainly in that mass transfer rates from the electrolyte to the surface become higher [29, 30]. However, altering the gas affects not only the O_2 content in the electrolyte but also the red–ox potential of the electrolyte. Figure 6a shows the OCP of the electrode in AO7 solution (2.5×10^{-5} mol L^{-1} + 0.1 mol L^{-1} Na_2SO_4) in the dark and with UV illumination. The OCP with Ar bubbling is more negative than that with O_2 bubbling. As the laser is switched on, the OCP shifts (as expected) to be more negative in all cases. It is important to note that the OCP under illumination with O_2 bubbling is at −350 mV, whereas the OCP with Ar bubbling is at −500 mV. This is particularly interesting when comparing these values to the flat band potential of TiO_2, which lies at around −400 mV (Ag/AgCl) for Na_2SO_4 electrolytes [31]. In other words, as illustrated in Fig. 6b, under Ar bubbling, accumulation conditions are established (ejecting electrons from the semiconductor surface to the electrolyte), while under O_2 saturation (expected) depletion conditions are established (ejecting holes from the semiconductor surface to the electrolyte). These experiments illustrate that the reaction rate cannot simply be explained by the O_2 content in the solution.

In order to eliminate potential shifts due to light illumination and thus clarify the picture, we carried out potentiostatic experiments. Figure 7 shows the influence of an applied voltage if photocatalytic degradation experiments are carried out in a photoelectrochemical cell. First, if the potential is set to U_{fb} that is at ~−400 mV, clearly a higher rate for the O_2-containing electrolyte is obtained. This indicates that, under these conditions, electron transfer from the semiconductor to the electrolyte is important. Second, it is clear that applying a mild positive bias drastically increases the decomposition rate of the organic dye for both O_2- and Ar-bubbled electrolytes. This can be straightforwardly explained by a higher band bending in the TiO_2 electrode with a positive bias, i.e., separation of electron–hole

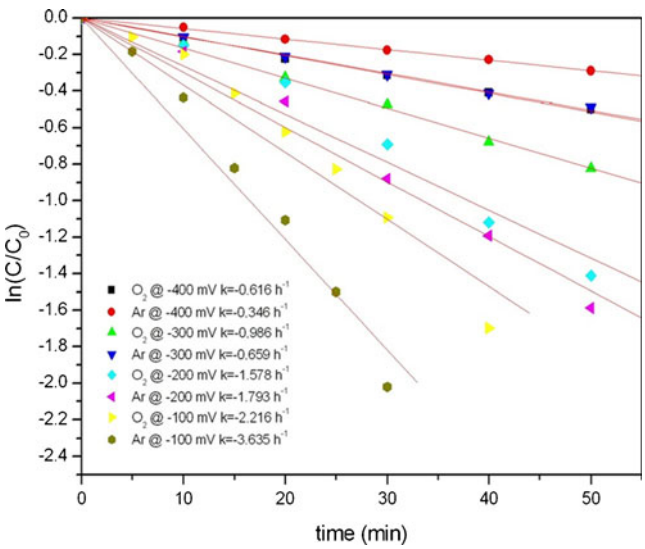

Fig. 7 Degradation curves of AO7 by TiO_2 nanotubes (annealed at 450 °C in air) with irradiation time of UV light with the applied potential ranging from −400 to −100 mV under different gas bubbling, Ar or O_2

pairs is faster and less recombination occurs. This leads to a higher hole transfer rate to the electrolyte, indicating that the valence band path now becomes rate-determining. Nevertheless, the voltage-induced enhancement of the reaction is much more pronounced for the Ar-bubbled electrolyte, i.e., at higher anodic voltages, a higher decomposition rate is obtained for the lower O_2 content in the electrolyte. This detrimental effect of O_2 in the electrolyte may be ascribed to parasitic pathways interfering with active destruction of the target organic molecule [4]. Overall, the electrochemical results show that the simple picture is: (1) under open-circuit conditions, the electron transfer reaction to O_2 is rate-determining and (2) under anodic bias, hole transfer to the red–ox species is rate-determining (does hold only partially). While similar concepts have been evaluated for TiO_2 nanoparticle electrodes [32, 33], the present work shows that detailed aspects of the experiments also need to be considered for TiO_2 nanotube photoelectrodes.

Conclusions

The goal of this investigation is to evaluate various crucial parameters on the photocatalytic activity of TiO_2 nanotube layers. We show that not only the annealing temperature and resulting anatase or rutile content but also the annealing atmosphere (and resulting Ti^{3+} states) are crucial. Furthermore, under open-circuit conditions, not only the O_2 content in the electrolyte but also light-induced changes in the equilibrium Fermi level need to be considered.

Under applied anodic bias, due to increased band bending, charge separation is more efficient and leads to enhanced hole-induced photocatalytic reactions. Nevertheless, we find that the presence of O_2 in the electrolyte at higher anodic potentials negatively affects the degradation rate of the organic dye (used as a model pollutant). In general, the results address a number of critical issues that are frequently disregarded when performing photocatalytic experiments with TiO_2 nanotube layers.

Acknowledgments The authors acknowledge DFG, Engineering of Advanced Materials (Cluster of Excellence, University of Erlangen), for financial support and Ulrike Marten-Jahns for XRD measurements.

References

1. Fujishima A, Honda K (1972) Nature 238:37–38
2. Linsebigler AL, Lu G, Yates JT (1995) Chem Rev 95:735–758
3. Thompson TL, Yates JT Jr (2006) Chem Rev 106:4428–4453
4. Fujishima A, Zhang X, Tryk DA (2008) Surf Sci Rep 63:515–582
5. Paramasivam I, Jha H, Liu N, Schmuki P (2012) A review on photocatalysis using TiO_2 nanotubes and other ordered oxide nanostructures. Small
6. Macak JM, Zlamal M, Krysa J, Schmuki P (2007) Small 3:300–304
7. Dijkstra MFJ, Michorius A, Buwalda H, Panneman HJ, Winkelman JGM, Beenackers AACM (2001) Catal Today 66:487–494
8. Subramanian V, Kamat PV, Wolf EE (2003) Ind Eng Chem Res 42:2131–2138
9. Vinodgopal K, Hotchandani S, Kamat PV (1993) J Phys Chem 97:9040–9044
10. Vinodgopal K, Stafford U, Gray KA, Kamat PV (1994) J Phys Chem 98:6797–6803
11. Hoffmann MR, Martin ST, Choi W, Bahnemann DW (1995) Chem Rev 95:69–96
12. Mills A, Davies RH, Worsley D (1993) Chem Soc Rev 23:417–425
13. Zlamal M, Macak JM, Schmuki P, Krysa J (2007) Electrochem Commun 9:2822–2826
14. Song YY, Roy P, Paramasivam I, Schmuki P (2010) Angew Chem Int Ed 49:351–354
15. Lynch RP, Ghicov A, Schmuki P (2010) J Electrochem Soc 157: G76–G84
16. Fujishima A, Rao TN, Tryk DA (2000) J Photochem Photobiol C Photochem Rev 1:1–21
17. Fotou GP, Vemury S, Pratsinis SE (1994) Chem Eng Sci 49:4939–4948
18. Ohno T, Sarukawa K, Matsumura M (2001) J Phys Chem B 105:2417–2420
19. Gesenhues U (1994) Farbe Lack 100:244–247
20. Gerischer H, Heller A (1991) J Phys Chem 95:5261–5267
21. Schwitzgebel J, Ekerdt JG, Gerischer H, Heller A (1995) J Phys Chem 99:5633–5638
22. Wang D, Liu L, Zhang F, Tao K, Pippel E, Domen K (2011) Nano Lett 11:3649–3655
23. Kiriakidou F, Kondarides DI, Verykios XE (1999) Catal Today 54:119–130
24. Roy P, Berger S, Schmuki P (2011) Angew Chem Int Ed 50:2904–2939
25. Kho YK, Iwase A, Teoh WY, Madler L, Kudo A, Amal R (2010) J Phys Chem C 114:2821–2829
26. Tighineanu A, Ruff T, Hahn R, Schmuki P (2010) Chem Phys Lett 494:260–263
27. Diebold U (2003) Surf Sci Rep 48:53–229
28. Liu N, Albu SP, Lee K, So S, Schmuki P (2012) Water annealing and other low temperature treatments of anodic TiO_2 nanotubes: a comparison of properties and efficiencies in dye sensitized solar cells and for water splitting. Electrochim Acta
29. Hamann CH, Vielstich W (1998) Elektrochemie. Wiley, Weinheim
30. Plieth W (2008) Electrochemistry for materials science. Elsevier, UK
31. Taveira LV, Sagues AA, Macak JM, Schmuki P (2008) J Electrochem Soc 155:C293–C302
32. Salvador P, Gutierrez C (1984) J Phys Chem B 88:3696–3698
33. Salvador P (1985) J Phys Chem B 89:3863–3869